Functional Materials 17, No.4 (2010)

Growth and optical properties of $Al_2O_{3-\delta}:N_x$ crystals

Kh.Sh.-ogly Kaltaev, N.S.Sidelnikova, S.V.Nizhankovsky, A.Ya.Dan'ko, A.T.Budnikov

Institute for Single Crystals, STC "Institute for Single Crystals",
National Academy of Sciences of Ukraine,
60 Lenin Ave., 61001 Kharkiv, Ukraine

Received May 31, 2010

The formation conditions of the $Al_2O_{3-\delta}:N_x$ solid solution at the sapphire crystal growing in nitrogen-containing reducing atmospheres of different compositions have been studied. It has been shown that the Al_2O_3 interaction with a nitrogen-containing medium of a low oxygen potential ($P_{O_2}<P^S_{O_2}$) (Al_2O_3) is accompanied, along with the Al_2O_3 violation, by nitrogen incorporation into the oxygen sublattice of anion-defect corundum and formation of a $Al_2O_{3-\delta}:N_x$ solid solution having the corundum structure. The nitrogen dissolution in sapphire has been established to be accompanied by the formation of F^+ centers and aggregative F_2 ones; those defects influence considerably the sapphire optical characteristics.

Исследованы условия образования твердого раствора $Al_2O_{3-\delta}:N_x$ при выращивании кристаллов сапфира в азотсодержащих восстановительных средах различного состава. Показано, что взаимодействие Al_2O_3 со средой, характеризующейся низким кислородным потенциалом ($P_{O_2}<P^S_{O_2}$) (Al_2O_3) и содержащей азот, наряду с нарушением стехиометрии Al_2O_3, сопровождается встраиванием азота в кислородную подрешетку анион-дефектного корунда с образованием раствора $Al_2O_{3-\delta}:N_x$ со структурой корунда. Установлено, что процесс растворения азота в сапфире сопровождается образованием F^+-центров и агрегатных F_2-центров, дефектов, которые оказывают существенное влияние на оптические характеристики сапфира.

1. Introduction

Optical properties of sapphire, as well as of other crystalline dielectrics, are defined considerably by the intrinsic and extrinsic defects present therein. The defects responsible for the absorption and luminescence bands in UV and visual range include the anionic and cationic vacancies (F and V centers, respectively) an the agglomerates thereof formed due to ionizing irradiation and different heat treatments, as well as the impurity centers (Fe, Si, Mg, Ti, Co, Cr, etc.) substituting for the Al^{3+} ions in cationic positions. The presence of foreign impurity ions in the Al_2O_3 lattice may also affect appreciably both the valence and concentration of intrinsic defects [1]. The energy characteristics of such processes are considered in literature in detail [2–5]. There are no data on purposeful studies of similar processes accompanying the dissolution of impurities (nitrogen in particular) in the anionic corundum sublattice. Such investigations are of a great interest for various applications of sapphire, in particular, in connection with nitriding mechanism of sapphire substrate surfaces and formation of an interlayer necessary for the subsequent deposition of heterostructures based on AlN–GaN and InN–GaN solid solutions. This process consists essentially in forma-

tion of an AlN_xO_{1-x} or AlN film using an anneal in a medium containing a nitrogen-bearing component (usually NH_3) as well as a plasma treatment or ion implantation [6–9]. Although the nitriding is used widely to obtain various high-quality materials on sapphire, the process mechanism (especially of its initial stage preceding the Al_2O_3–AlN_xO_{1-x} or Al_2O_3–AlN phase transformations) is studied inadequately to date.

2. Theoretical calculations

Recently, a novel technique has been proposed to nitridize sapphire and to obtain the AlON and AlN films using the annealing in a nitrogen-containing reducing atmosphere (N_2+CO+H_2) being a gaseous N_2, CO, CO_2, H_2, H_2O mixture at very low CO_2 ang H_2O concentrations [10–11]. When studying the film formation mechanism, it has been found using the XPS technique that an increased nitrogen concentration in a sample bearing the AlN film (as compared to the reference sapphire sample, i.e., the initial substrate) is observed at a depth exceeding considerably the film thickness determined by X-ray study [12]. At the same time, the optical absorption (OA) spectrum of the sapphire substrate shows an increased intensity of the band associated with the F center presence (6.05 eV) and a band at 4.8 eV appears associated with the F^+ centers. The reduction of nominally pure sapphire crystals is known to result mainly in the formation of neutral F centers. The concentration increase can be attained either by irradiation with high-energy particles or in the presence of a relatively high concentration of impurities having a failing positive charge (Me^{2+}:Fe, Mg, etc.). In the latter case, the F^+ center formation is caused by the necessity to keep the electric neutrality [1–5]:

$$Al_2O_3 + Me^{2+} \longleftrightarrow \left(2Me^{2+}_{Al} + V_O\cdot\right)^x, \qquad (1)$$

where Me^{2+} is an impurity atom in the Al position; $V_O^{\bullet}$, an oxygen vacancy with one trapped electron (F^+ center). The index x characterizes the molecular neutrality. It can be supposed (by analogy with other oxides, in particular, HfO_2, TiO_2, ZrO_2 [13–15]) that the nitrogen incorporation into vacant anionic positions in the corundum structure gives a similar result:

$$V_O + N^{3+} \longleftrightarrow \left(N^{3+}_O + V_O\cdot\right)^x, \qquad (2)$$

where V_O is an oxygen vacancy with two trapped electrons (F center); N_O^{3+}, nitrogen in an oxygen position.

The supposed mechanism of an AlN film formation at the sapphire surface during the annealing in a nitrogen-containing reducing atmosphere, that provides a reasonable interpretation of experimental data, can be subdivided conventionally into two stages. Initially, the stoichiometry violation of the surface layer occurs and the nitrogen diffusion into sapphire depth (that is favored by the presence of vacant sites in the corundum anionic sublattice). This is accompanied by formation of an $Al_2O_{3-\delta}$:N_x solid solution (having the corundum structure) in the diffusion region. If the medium composition provides the AlN phase existence conditions, then as a certain critical solution composition is attained, an AlN film is formed in a layer much thinner than the diffusion region. Otherwise, according to the mechanism mentioned, the nitriding in the N_2+CO+H_2 atmosphere results only in an $Al_2O_{3-\delta}$:N_x solid solution and is not accompanied by the $Al_2O_3 \rightarrow$ AlN phase transformations. The same is valid for the formation of an AlON film (or an AlON–AlN phase mix).

Thermodynamical consideration of the reduction and nitriding processes has been carried out for a gas atmosphere comprising nitrogen and CO as the reducing component. The non-stoichiometry appears due to mass exchange between Al_2O_3 and envorinment in a medium with a low oxygen potential where the oxygen partial pressure is lower than that above stoichiometric Al_2O_3 ($P^S_{O_2}(Al_2O_3)$). The concentration of neutral anionic vacancies (C_V) is related to the oxygen pressure in the vapor phase as

$$C_V = K_V \cdot \left(P_{O_2}\right)^{-1/2}, \qquad (3)$$

where K_V is the equilibrium constant of the reaction

$$O_O \longleftrightarrow V_O + 1/2O_2(g). \qquad (4)$$

In a CO–CO_2 gas phase, the oxygen partial pressure in the gas phase (i.e., its oxygen potential) is defined by the P_{CO_2}/P_{CO} ratio:

$$P_{O_2} = \left(K \cdot P_{CO_2}/P_{CO}\right)^2, \qquad (5)$$

where K is the equilibrium constant of the reaction

$$CO_2 \longleftrightarrow CO + \tfrac{1}{2}O_2. \qquad (6)$$

Therefore, the existence regions of stiochiometric Al_2O_3 and the anion-defect corundum ($Al_2O_{3-\delta}$) in a $CO–CO_2$ gas mixture can be defined in the T, P_{CO_2}/P_{CO} coordinates.

The AlON and AlN existence regions in a $N_2+CO+CO_2$ gas mixture are restricted by the equilibrium conditions ($\Delta G=0$) for the formation reactions of γ-AlON:

$$[(64 + x)/3x]Al_2O_3(s) + 3CO(g) + N_2(g) = (2/x)Al_{(64+x)/3}O_{32-x}N_x + 3CO_2(g), \quad (7)$$

and of AlN:

$$Al_2O_3(s) + 3CO(g) + N_2(g) = 2AlN(s) + 3CO_2(g), \quad (8)$$

and thus can be defined, using the equilibrium constants for those reactions, in the T, P_{CO_2}/P_{CO}, P_{N_2}2 coordinates. The condition $\Delta G<0$ for the reactions (7), (8) must be valid also for the existence of an AlON or AlN film formed at the solid-phase reactions between nitrogen and an anion-defect corundum (otherwise, the compounds would be decomposed according to the reverse reactions). The corresponding estimations of the $T–P_{CO_2}/P_{CO}$ relationships that separate the existence regions of Al_2O_3 and $Al_2O_{3-\delta}$ as well as the $T–P_{CO_2}/P_{CO}–P_{N_2}$ ones restricting the AlON and AlN existence regions within the 1200–2200°C temperature range are presented in the diagram, Fig. 2. As to γ–AlON, the calculation has been done for the $(AlN)\cdot 3(Al_2O_3)$ composition:

$$7Al_2O_3(s) + 3CO(g) + N_2(g) = 2(AlN \cdot 3Al_2O_3(s) + 3CO_2(g). \quad (9)$$

In the calculations, used were the formation energy values for AlN: $\Delta G°(AlN)=-316.2+0.1157\cdot T$ [16],

$$(AlN)\cdot 3(Al_2O_3):\Delta_f G°(Al_7O_9N) = -5315.2132 + 1.054520\cdot T \text{ [17]},$$

as well as the reference data [18].

It follows from the calculations that as the temperature rises, the limiting value of P_{CO_2}/P_{CO} corresponding to $P_{O_2}=P^S_{O_2}(Al_2O_3)$ increases from $1.7\cdot 10^{-3}$ at 1200°C to $2.4\cdot 10^{-2}$ at 2200°C. Much lower P_{CO_2}/P_{CO} values are required for the AlON and AlN existence. So at the nitrogen pressure near the atmospheric one, the existence region thereof is limited by the P_{CO_2}/P_{CO} values of $<10^{-5}$ at 1200°C and $<10^{-4}$ at 2200°C, that correspond to the molecular oxygen partial pressures in the gaseous medium of $<10^{-18}$ Pa and $<10^{-8}$ Pa, respectively. Even more considerable reduction of P_{CO_2}/P_{CO} is required at lower P_{N_2} values. In the diagram, the region where the AlON and AlN cannot exist but where the P_{CO_2}/P_{CO} values correspond to $P_{O_2}<P^S_{O_2}(Al_2O_3)$ is shown as that of the $Al_2O_{3-\delta}$:N solid solution existence.The solution composition can be supposed to depend both on the Al_2O_3 stoichiometry violation degree and on the nitrogen partial pressure in the in the medium.

3. Experimental

The formation possibility of the $Al_2O_{3-\delta}$:N_x solid solution due to nitrogen dissolution in anion-defect corundum was studied in experiments on the sapphire crystal growing in nitrogen-containing atmospheres of different compositions. The crystals were grown by horizontal directional crystallization (HDC) using the carbon-graphite heat insulation [19, 20]. The carbon present in the heating zone provides a gas atmosphere with a low oxygen partial pressure that is a reducing one for Al_2O_3. The crystals were grown both at P_m about 6.7 to 40 Pa (under rough evacuation) and at 106 to 126 kPa in a closed chamber. In the first case, the gas medium consists essentially of CO and H_2 mix (P_{H_2}/P_{CO} ~0.02–0.04). The main residual gas component in the crystallization chamber is nitrogen, its concentration after a standard evacuation being about 0.1 to 0.4 vol. %. To increase the nitrogen concentration in the growing atmosphere, an additional buffer gas (nitrogen or air) flow was used during the evacuation, thus riding the nitrogen concentration up to 20–40 vol. %.

When crystallizing in the closed volume, the pre-evacuated chamber at the residual pressure of about 13 to 40 Pa was filled with Ar, N_2, or a mixture thereof up to 106 to 126 kPa pressure. In this case, the total concentration of reducing components ($CO+H_2$) formed due to the adsorbed oxygen and water varor interaction with the carbon-graphite materials is about 1 to 5 vol %, depending on the pre-evacuation. The N_2, CO, and H_2 concentrations in the gas atmosphere was monitored using a Kristall 2000M gas chromatograph. The optical density of samples was measured using a Perkin-Elmer Lambda-35 spectrophotometer in

the wavelength range of 190 to 1100 μm. Prior to measuring the spectrum (2), the about 50 μm thick AlN film obtained under the nitriding was removed by a mechanical polishing. Thereafter, the absence of AlON and AlN phases in the surface layer was checked using XPA.

To obtain the thermostimulated luminescence (TSL) curves, the samples were irradiated in air at 295 K with X-rays (Cu anode, 40 kV, 10 mA) for 70 min and then heated up to 330°C at a constant rate of 1°C/s. The TSL curves were measured using an automated setup including a FEU-106 PMT operated in the photon counting mode. To determine the TSL spectral composition, the absorption light filters with a known transmission band (SS15, λ = 330 to 480 nm, or OS12, λ > 560 nm) were placed between the sample and the PMT. A nitrogen laser (the pulse duration about 8 ns, the maximum power 5 kW, the wavelength 337 nm) was used as the excitation source. The spectrum was recorded in the 440 to 750 nm using a diffraction spectrometer provided with a PZS matrix.

4. Results and discussion

In the diagram, Fig. 1, the atmosphere composition in the supposed existence region of the $Al_2O_{3-\delta}:N_x$ solution (P_{CO_2}/P_{CO} and P_{N_2}<~ kPa) corresponding to the crystal growth conditions is shown by arrows. In the diagram, the P_{CO_2}/P_{CO} value is shown that is defined by the equilibrium of the carbon gasification reaction:

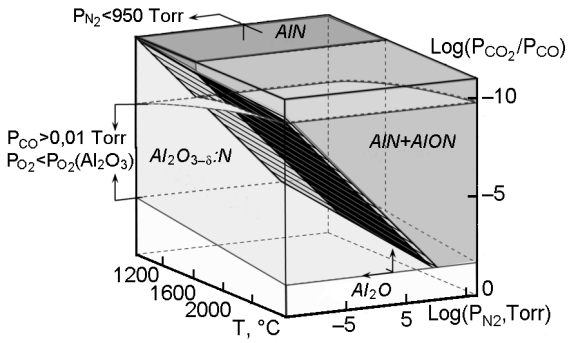

Fig. 1. Dependence of the Al_2O_3–$Al_2O_{3-\delta}$:N–AlON–AlN system composition on T, P_{CO2}/P_{CO}, P_{N2} in the $CO+N_2$ atmosphere.

$$C + CO_2 \longleftrightarrow 2CO, \qquad (10)$$

at P_{CO} = 1.33 Pa. That is the minimum P_{CO_2}/P_{CO} value possible to be attained in the experiments, as the gas saturation of the carbon-graphite heat insulating materials does not allow to provide the residual pressure in the chamber lower than 1.33 Pa. In fact, the P_{CO_2}/P_{CO} ratio exceeds that corresponding to the equilibrium conditions of reaction (10) and is defined by the crystallization chamber design, in particular, by the surface area ratio of the graphite shields and the melt, the graphite-to-melt distance, the graphite regeneration ability, the convection features inside the chamber, etc. The growing conditions of the experimental crystals are listed in Table 1.

It was found before [20] that the optical characteristics of sapphire grown by HDC

Table 1. Crystal growing conditions

Sample	P_m, kPa	Atmosphere composition	C_{CO+H_2}, vol. %	P_{CO+H_2}, kPa	C_{N_2}, vol. %	P_{N_2}, kPa	Nitrogen-containing mixture
1	0.026	$CO+H_2$	99	0.026	<0.5	–	None
2*	0.026	$CO+H_2+N_2$	75	0.02	25	0.0066	Air
3*	0.026	$CO+H_2+N_2$	60	0.016	40	0.011	Nitrogen
4	0.026	$CO+H_2+N_2$	70	0,14	30	0.008	Air
5	13.3	$Ar+CO+H_2$	5	0.66	0.2	0.026	None
6	10.66	$Ar+CO+H_2+N_2$	10	1.066	40	4.26	Ar+air
7	106	$Ar+CO+H_2$	1	1.066	0.1	0.106	None
8	950	$Ar+CO+H_2+N_2$	1	0.168	1	1.266	Ar+Nitrogen
9	126	$Ar+CO+H_2+N_2$	1	0.168	10	12.66	Ar+Nitrogen
10	126	N_2+CO+H_2	1	0.168	99	124.1	Nitrogen

* when growing the crystals 2*, 3*, tungsten heat shield was placed above the melt.

using the carbon-graphite heat insulation from a raw material with basic impurity content up to 100 ppm are defined mainly by the partial pressure of reducing components in all the crystallization process stages as well as by the polyvalent Ti impurity in the raw material. The relation of those parameters defines the dominant defect type (anionic vacancies, i.e. neutral F centers, or Ti^{4+} impurity ones) that define the crystal optical properties. If the growing conditions do not provide the transition of a considerable fraction of Ti impuity to the Ti^{3+} charge state $((V_O^{++} + 2e) + Ti^{4+} \rightarrow (V_O^{++} + e) + Ti^{3+})$, then the crystals show a reduced transparence in the 200–300 nm range (the spectral region corresponding to the Ti^{4+} absorption). Otherwise, mainly the absorption bands of neutral F centers (at 205 nm) are observed in the OA spectrum, its intensity being defined by the reducing component ($CO+H_2$) partial pressure. The contribution from the F^+ centers is relatively small and usually does not exceed 10 % of the total amount of anionic defects. In Fig. 2, compared are the OA spectra of such crystals (1, 5, 7 in Table 1) and those grown in reducing atmospheres vith nitrogen concentrations exceeding 0.5 vol. %. Table 2 shows the F and F^+ center concentrations (C_F, C_F^+, respectively) as estimated after the $K(\lambda)$ spectra expansion into Gaussians using the Smacula formula

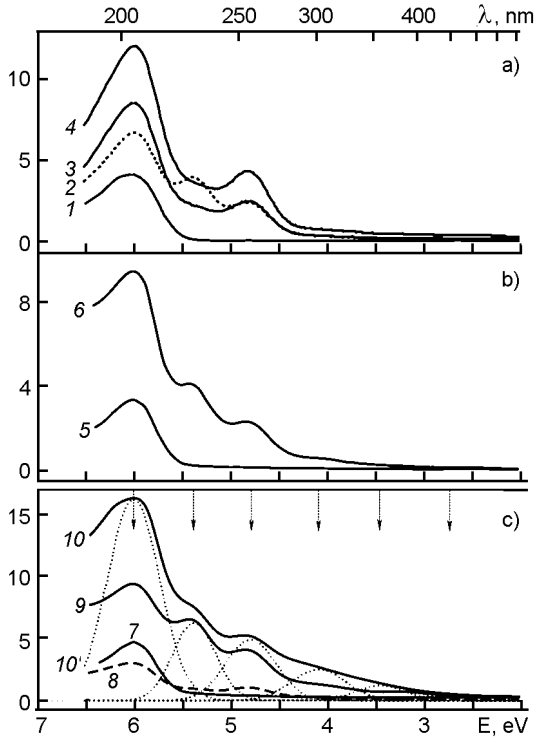

Fig. 2. OA spectra of sapphire grown in nitrogen-containing reducing atmospheres of different compositions at the pressure (P_m): about 26 Pa (a), 10 to 13 kPa (b); 106 to 126 kPa (c). The curve numbers in the Figure correspond to sample numbers in Table 1. 10′ is the spectrum 10 expansion into components.

$$C_F \cdot f = 0.87 \cdot 10^{17} \cdot n \cdot (2 + n^2)^{-2} \cdot K_{max} \cdot \Delta, \quad (11)$$

where C_F is the F or F^+ center concentration; K_{max}, the absorption coefficient maximum value; Δ, the peak full width at half intensity; n, the refractive index at the wavelength corresponding to K_{max}; f, the oscillator strength (f_F=1.3 and f_F^+=0.66 [21] were used in the calculations). The ex-

Table 2. F and F^+ center concentrations in sapphire samples grown in nitrogen-containing reducing atmospheres of different compositions

Sample	C_F	C_F^+ (5.4 eV)	C_F^+ (4.8 eV)	C_F^+/C_F
1	$8.9 \cdot 10^{15}$	$1.63 \cdot 10^{14}$	$8.1 \cdot 10^{13}$	0.03
2	$1.55 \cdot 10^{16}$	$1.41 \cdot 10^{16}$	$1.01 \cdot 10^{16}$	1.56
3	$1.99 \cdot 10^{16}$	$7.87 \cdot 10^{15}$	$1.04 \cdot 10^{16}$	0.92
4	$3.09 \cdot 10^{16}$	$1.18 \cdot 10^{16}$	$1.92 \cdot 10^{16}$	1.0
5	$7.2 \cdot 10^{15}$	$4.08 \cdot 10^{14}$	$5.2 \cdot 10^{14}$	0.13
6	$2.59 \cdot 10^{16}$	$1.15 \cdot 10^{16}$	$1.16 \cdot 10^{16}$	0.89
7	$8.31 \cdot 10^{15}$	$7.9 \cdot 10^{14}$	$8.81 \cdot 10^{14}$	0.2
8	$7.42 \cdot 10^{15}$	$2.04 \cdot 10^{15}$	$4.73 \cdot 10^{15}$	0.91
9	$2.37 \cdot 10^{16}$	$2.36 \cdot 10^{16}$	$1.88 \cdot 10^{16}$	1.79
10	$4.14 \cdot 10^{16}$	$2.72 \cdot 10^{16}$	$2.47 \cdot 10^{16}$	1.25

ample of the spectra expansion into component for spectrum 10 presented on Fig. 2.

The data from Fig. 2 and Tables 1, 2 show that independent of the growth atmosphere total pressure P_m, the increased nitrogen concentration therein results in increased intensities of the 4.8 and 5.4 eV absorption bands associated with the presence of F^+ centers. In the crystals grown in reducing atmospheres containing >0.5 vol. % nitrogen, the C_{F^+}/C_F ratio amounts 0.9 to 1.8, in contarst to ~0.1 in the standard crystals. Those data evidence the formation of the $Al_2O_{3-\delta}:N_x$ solution in those conditions. According to the reaction (2), the nitrogen concentration in the solution is about (2 to 5)·10^{16} cm^{-3}. The concentration of F^+ centers that characterizes the solution composition depends both on the nitrogen concentration in the atmosphere and on the reducing properties thereof. This is confirmed, in particular, by the change occurring as the tungsten heat shield above the melt is replaced by a graphite one (Samples 2, 3, 4).

Fig. 3 presents the OA spectra for the crystals grown under increase of the nitrogen concentration in the atmosphere at different crystallization stages. The crystals were grown in the following conditions.

Crystal I: the temperature elevation, the raw material pre-melting, and growing of a crystal part in standard conditions at P_m about 13 to 26 Pa (C_{N_2}<0.5 vol %), the rest of the crystal being grown at the pressure in the chamber increased to about 53 Pa using an additional air flow.

Crystal II: the temperature elevation and the raw material pre-melting at about 53 to 80 Pa using an additional air flow and the crystal growing in standard conditions at P_m about 13 Pa (C_{N_2}<0.5 vol. %).

The F and F^+ center concentrations are shown in Table 3.

It has been sbown before [20] that during the crystallization process under a forevacuum evacuation, the crystallization conditions vary from more reducing to less reducing ones due to the degassing of raw

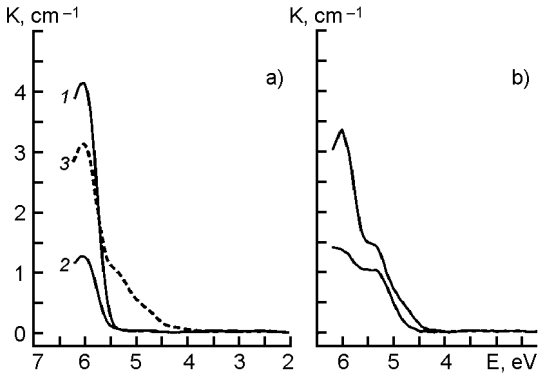

Fig. 3. OA spectra of the crystals with different parts grown at different conditions. (a) The samples are cut out from the crystal I initial (*1*), middle (*2*) and end (*3*) parts. (b) The samples are cut out from crystal II initial (*4*) and end (*5*) parts.

material, heat insulation, and the chamber walls. That variation results in the neutral F center concentration decrease from the crystal I initial part towards its middle. The F^+ center concentration in that crystal part is rather low. As the atmosphere pressure increases when the crystal is grown in the part 3 due to the air flow (that is accompanied both by the atmosphere reducing properties increase and the nitrogen concentration therein rises), a significant increase in C_{F^+} is observed. Whereas in the crystal II grown in the same conditions as the parts 1 and 2 of the crystal I, the decrease of the F^+ center concentration is less pronounced, while that of the F center is lowered substantially from the initial crystal part towards its end (Table 3). The fact that the nitrogen concentration in the $Al_2O_{3-\delta}:N_X$ solution formed during the raw material premelting does not decrease substantially even when the crystal is grown in an atmosphere with a low (<0.5 vol %) nitrogen concentration confirms its rather high stability.

Besides of intense absorption bands of F^+ centers, the OA spectra of $Al_2O_{3-\delta}:N_X$ crystals include additional bands in the 3 to

Table 3. F and F^+ center concentrations in sapphire samples

Sample	C_F	C_{F^+} (5.4 eV)	C_{F^+} (4.8 eV)	C_{F^+}/C_F
1	$8.9\cdot10^{15}$	$1.63\cdot10^{14}$	$8.0\cdot10^{13}$	0.03
2	$2.77\cdot10^{15}$	$1.63\cdot10^{14}$	$2.28\cdot10^{14}$	0.14
3	$7.74\cdot10^{15}$	$3.3\cdot10^{15}$	$1.92\cdot10^{15}$	0.68
4	$8.12\cdot10^{15}$	$4.84\cdot10^{15}$	$1.91\cdot10^{15}$	0.83
5	$2.99\cdot10^{15}$	$5.51\cdot10^{15}$	$4.4\cdot10^{14}$	1.99

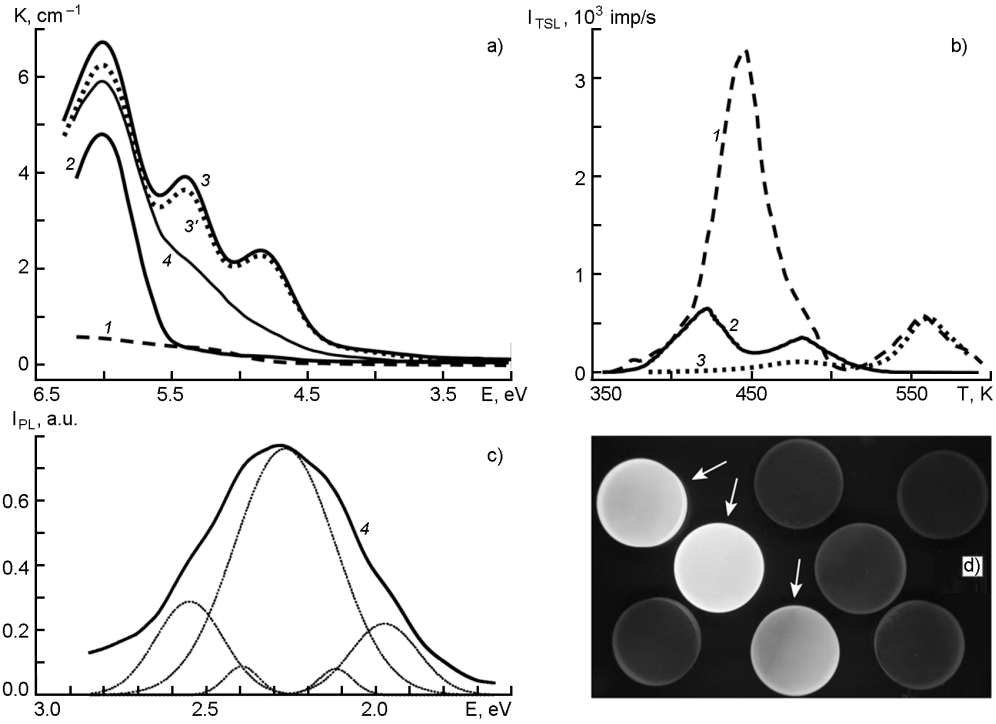

Fig. 4. (a) OA spectra, (b) TSL curves and (c) PL spectrum of sapphire grown in reducing atmospheres of various compositions and pressures. The curve numbers in the Figure correspond to the sample numbers in Table 4. 3′ is the spectrum 3 change after UV irradiation. (d) Photoluminescence of $Al_2O_{3-\delta}:N_x$ samples (shown by arrows) during N_2 laser irradiation as compared to the standard $Al_2O_{3-\delta}$ crystals.

4 eV range causing a more or less intense yellow color therein. Those bands can be ascribed preliminarily to the presence of aggregative F_2 centers, i.e., oxygen bivacancies with four, three, or two trapped electrons (F_2, F_2^+, and F_2^{2+} centers), that are identified by the optical absorption at 4.09, 3.47, and 2.75 eV, respectively (Fig. 2c). These defects are formed both in nominally pure sapphire crystals under high irradiation doses and at high concentrations of impurities having a failing positive charge [22–27]. The presence of absorption bands in that region causes, in particular, the yellow color of sapphire crystals containing Mg impurity [2, 28]. The absorption bands in the 3–4 eV region may be associated also with the formation of N_O–O^--defects with charge transferbetween oxygen and nitrogen in oxygen site. The formation possibility of similar complexes (Mg_{Al}–O^-) believed to be associated with the absorption bands at 2.65 and 3.26 eV has been considered in connection with Mg dissolution in Al_2O_3 [2].

Along with a significant effect of nitrogen dissolution on the OA spectra of sapphire grown in nitrogen-containing reducing atmospheres, a change in its luminescence characteristics is observed, too. Fig. 4 shows the OA spectra, the thermostimulated luminescence curves and the photoluminescence (PL) ones for sapphires

Table 4. Crystal growing conditions

Sample	P_m, kPa	Atmosphere composition	Nitrogen-containing mixture	Concentration, vol. %		
				Ar	N_2	$CO+H_2$
1	0.0066	$CO+H_2$	None	–	0.2	>99
2	53.3	$Ar+CO+H_2$	None	≈95	0.1	3–5
3	0.04	$CO+H_2+N_2$	Air	–	30	70
4	0.026	$CO+H_2+N_2$	Air	–	30	70

grown in atmospheres of different composition and pressure. The crystal growth conditions are presented in Table 4. Fig. 4d shows also photos of sapphire samples cut out from the standard crystals grown at P_m~13–26 Pa (C_{N_2}<0.5 vol. %) and from $Al_2O_{3-\delta}$:N crystals (indicated by arrows) grown at P_m~26 Pa (C_{N_2}<20–30 vol. %) under irradiation with a wide beam of a nitrogen laser (λ = 337 nm).

As noted above, the optical characteristics of sapphire grown by the HDC technique in reducing conditions at a nitrogen concentration in the atmosphere <0.5 vol. % are defined mainly by the partial pressure of reducing components at all the crystallization process stages and by the concentration of polyvalent Ti impurity. Depending on the relation of those parameters, either the Ti^{4+} absorption bands (Fig. 4a, curve *1*) or those of neutral F centers (Fig. 4a, curve *2*) prevail in the OA spectra of the crystals, a correlation between the OA spectra and TSL curves being observed [20, 29] (Fig. 4b).

For the crystals with dominating F center absorption bands, the TSL curves show the prevailing peaks at 152 and 207°C associated with the anionic defects and the Ti^{3+} impurity, respectively. For the crystals with predominating Ti^{4+} absorption bands, peaks at 167 and 287°C are also present. The 152 and 207°C are not expressed explicitly but their presence is evidenced by peculiarities in the ascending and descending branches of the more intense peak at 167°C. The 167 and 287°C peaks in those crystals are associated most likely with the Ti^{4+} impurity as well as with complexes including oxygen vacancies and Ti^{4+} ions.

At the same time, though the OA spectra of $Al_2O_{3-\delta}$:N_x crystals (curves *3*, *4*) contain intense absorption bands of F centers, the TSL curve (Fig. 4b, curve *3*) does not include the peak with T_{m1} = 152°C that could be ascribed to the presence of F centers (at λ = 420 nm). In contrast, only the peak with T_{m3} = 207°C associated with the Ti^{3+} center is visible as well as that with T_{m4} = 287°C that is not observed in the crystals with dominating F center absorption bands in the OA spectrum (curve *2*) associated with the F center- Ti^{4+} complex.

This result could be explained when considering the OA spectrum changes due to UV irradiation. According to common concepts, the free electrons formed in the course of F center ionization under irradiation may be trapped in traps of various depth; this process is accompanied by the $F \rightarrow F^+$ center conversion. The luminescence of F centers (420 nm) corresponds to the inverse transition $F^+ + e^- \rightarrow F^* \rightarrow F + h\nu_{420nm}$ [30]. After the thermal luminescence and trap emptying, the OA spectra return to their initial shapes (being observed prior to irradiation). Such a behavior (an absorption decrease in the F center region and increase in the F^+ center one under UV irradiation and the spectrum restoration after thermal luminescence) is typical of the anion-defect corundum $Al_2O_{3-\delta}$ and was observed in our works [20] as well as by other reseachers [31–33]. In contrast, such a behavior is nonrelevant for $Al_2O_{3-\delta}$:N_x crystals. In Fig. 4a, presented are the OA spectra for a crystal grown in a medium containing about 30 vol. % nitrogen prior to (3) and after (3′) irradiation with the full emission spectrum of a PRK-4 tube at 200 W power during 30 min. When comparing the spectra, it is seen that the irradiation does not cause the $F \rightarrow F^+$ center conversion. Thus, there are no preconditions for the $F^+ \rightarrow F$ transition associated with the T_{m1} = 152°C peak in the TSL curve. This seems to be connected with the fact that the F^+ centers (present in such crystals at high concentrations) predominate over other competing traps.

The intense photoluminescence in the visible spectral region at room temperature (Fig. 4c, d) is another specific feature of the $Al_2O_{3-\delta}$:N_x crystals. The PL spectrum shows a maximum intensity at 2.25–3.3 eV and is not elementary, that is evidenced by peculiarities in both spectrum branches. The positions of peaks at about 2.6, 2.4, and 2.27 eV coincides with literature data on the photoluminescence of aggregative F_2 centers (F_2^+, F_2, and F_2^{2+} centers, respectively) in the irradiated sapphire [22, 34] and Al_2O_3:Mg crystals [26, 27]. These data confirm the supposition that the absorption bands in the 3 to 4 eV range in the OA spectra of $Al_2O_{3-\delta}$:N_x crystals are due to the presence of aggregative F_2 centers.

5. Conclusions

Thus, the studies carried out have shown that the Al_2O_3 interaction with a nitrogen containing gas atmosphere having a low oxygen potential ($P_{O_2} < P^S_{O_2}(Al_2O_3)$) is accompanied, along with the Al_2O_3 stoichiometry violation, by nitrogen incorporation into oxygen sublattice of anion-defect corundum with formation of $Al_2O_{3-\delta}$:N_x solid solution having the corundum structure. The dissolution process is accompanied by formation of

F^+ centers and aggregative F_2 ones that are defects influencing significantly the sapphire optical characteristics.

References

1. P.Kofstad, High-temperature Oxidation of Metals, John Wiley and Sons. Inc., New York-London-Sydney (1966).
2. S.K.Mahapatra, F.A.Kroger, *J.Amer.Ceram. Soc.*, **60**, 141 (1977).
3. S.K.Mahapatra, F.A.Kroger, *J.Amer.Ceram. Soc.*, **61**, 106 (1978).
4. M.M.El-Aiat, F.A.Kroger, *J.Amer.Ceram. Soc.*, **65**, 162 (1982).
5. F.A.Kroger, *J.Amer.Ceram.Soc.*, **66**, 730 (1983).
6. P.Vennegues, B.Beaumont, *Appl.Phys.Lett.*, **75**, 4115 (1999).
7. F.Dwikusuma, T.F.Kuech, *J.Appl.Phys.*, **94**, 5656 (2003).
8. J.L.Deiss, Ch.Hirlimann, J.L.Loison et al., *Mater.Sci.and Engn.*, **B82**, 68 (2001).
9. Y.S.Cho, E.K.Koh, Y.J.Park et al., *J.Cryst. Growth*, **236**, 538 (2002).
10. A.Ya.Dan'ko, M.A.Rom, N.S.Sidelnikova et al., *Functional Materials*, **14**, 460 (2007).
11. Kh.Sh-o.Kaltaev, N.S.Sidel'nikova, S.V.Nizhankovskiy et al., *Semiconductors*, **43**, 1606 (2009).
12. Kh.Sh-o.Kaltaev, N.S.Sidel'nikova, M.A.Rom et al., in: Abstr. 7th All-Russian Conf. on Ga, In, and Al Nitrides: Structures and Devices, Moscow (2010), p.216.
13. K.Xiong, J.Robertson, S.J.Clark, *J.Appl. Phys.*, **99**, 044105-1 (2006).
14. A.V.Emeline, V.N.Kuznetsov, V.K Rybchuk, N.Serpone, *Int.J.Photoenergy*, **2008**, Art. ID 258394 (2008).
15. C.Reimann, T.Bredow, *J.Mol. Struct.:THEOCHEM*, **903**, 89 (2009).
16. W.Nakao, H.Fukuyama, K.Nagata, *J.Am. Ceram.Soc.*, **85**, 889 (2002).
17. X.Wang, W.Li, S.Seetharaman, *Scand.J. Metallurgy*, **31**, 1 (2002).
18. Thermodynamical Properties of Individual Compounds: A Reference Book, ed. by L.V.Gurvich et al., Nauka, Moscow (1981) [in Russian].
19. Ukrainian Patent 18923A (1993)
20. A.Ya.Dan'ko, V.M.Puzikov, V.P.Semynozhenko, N.S.Sidelnikova. Technological Principles of Sapphire Crystal Grown in Reducing Medium. ISMA, Kharkiv (2009) [in Russian].
21. B.D.Evans, M.Stapelbroek, *Phys.Rev.B*, **18**, 7089 (1978).
22. H.Nagabhushana, B.Umesh, B.M.Nagabhushana et al., *Spectrochim.Acta Part A*, **73**, 637 (2009).
23. K.Moritani, Y.Teraoka, I.Takagi et al., *J. Nucl.Mater.*, **373**, 157 (2008).
24. Y.Song, Q.Liu, Y.Sun et al., *Nucl.Instr.and Meth. Phys.Res.*, **B254**, 268 (2007).
25. V.E.Pelenyov, V.S.Kortov, I.I.Milman, *Radiat. Meas.*, **33**, 629 (2001).
26. R.Ramirez, M.Tardio, R.Gonzalez, J.E.M.Santiuste, *J.Appl.Phys.*, **101**, 123520 (2007).
27. S.Sanyala, M.S.Akselrod, *J.Appl.Phys.*, **98**, 033518 (2005).
28. J.Kvapil, B.Perner, J.Sulovski, Jos.Kvapil, *Krist.und Techn.*, **8**, 247 (1973).
29. I.Blonskyy, A.Vakhnin, A.Danko et al., *Semicond.Phys., Quant.Electronics & Optoelectronics*, **5**, 420 (2002).
30. K.H.Lee, J.H.Crawford Jr., *Phys.Rev.*, **19**, 3217 (1979).
31. V.S.Kortov, I.I.Milman, S.V.Nikiforov, V.E.Pelenyov, *Fiz.Tverd.Tela*, **45**, 1202 (2003).
32. I.I.Milman, V.S.Kortov, S.V.Nikiforov, *Fiz. Tverd.Tela*, **40**, 229 (1998).
33. I.A.Weinstein, V.E.Pelenyov, *Radiat. Meas.*, **38**, 421 (2004).
34. K.R.Nagabhushana, B.N.Lakshminarasappa, G.T.Chandrappa et al., *Radiat.Effects & Defects in Solids*, **162**, 325 (2007).

Вирощування та оптичні властивості кристалів $Al_2O_{3-\delta}:N_x$

Х.Ш-огли Калтаєв, Н.С.Сідельникова, С.В.Ніжанковський, О.Я.Данько, О.Т.Будніков

Досліджено умови утворення твердого розчину $Al_2O_{3-\delta}:N_x$ при вирощуванні кристалів сапфіру в азотовмісних відновних середовищах різного складу. Показано, що взаємодія Al_2O_3 з середовищем, яке характеризується низьким кисневим потенціалом ($P_{O_2}<P^S_{O_2}$) (Al_2O_3) та містить азот, разом з порушенням стехіометрії Al_2O_3, супроводжується входженням азоту до кисневої підгратки аніон-дефектного корунду з утворенням розчину $Al_2O_{3-\delta}:N_x$ зі структурою корунду. Встановлено, що процес розчинення азоту у сапфірі супроводжується утворенням F^+-центрів та агрегатних F_2-центрів-дефектів, які значно впливають на оптичні характеристики сапфіру.